A MULTIAXIAL THEORY OF VISCOPLASTICITY

FOR ISOTROPIC MATERIALS

D.N. Robinson and J.R. Ellis
The University of Akron
Akron, Ohio

INTRODUCTION

Many viscoplastic constitutive models for high-temperature structural alloys are based exclusively on uniaxial test data. Generalization to multiaxial states of stress is made by assuming the stress dependence to be on the second principal invariant (J_2) of the deviatoric stress, frequently called the "effective" stress. Testing other than uniaxial, e.g., shear, biaxial, etc., is generally done in the spirit of verification testing, not as part of the data base of the model.

If such a J_2 theory, based on uniaxial testing, is called upon to predict behavior under conditions other than uniaxial, say pure shear, and it does so poorly, nothing is left to adjust in the theory. The exclusive dependence on J_2 must be questioned.

For a fully isotropic material whose inelastic deformation behavior is relatively independent of hydrostatic stress, the most general stress dependence is on the two (non-zero) principal invariants of the deviatoric stress, J_2 and J_3. These invariants constitute what is known as an integrity basis for the material.

Here, we present a time-dependent constitutive theory with stress dependence on J_2 and J_3 that reduces to a known J_2 theory as a special case. The characterization of viscoplasticity can be made largely on uniaxial testing but the "strength" of the J_3 dependence must be determined by testing other than uniaxial, e.g., pure shear.

Earlier studies (refs. 1-3) have considered the inclusion of the invariant J_3 in the context of time-independent plasticity theory. The present time-dependent formulation is guided by the form of the yield function introduced in reference 1.

STATEMENT OF THE THEORY

As in references (4-6) the starting point is the assumed existence of a dissipation potential function

$$\Omega(\sigma_{ij}, \alpha_{ij})^*$$ (1)

with the generalized normality structure

$$\dot{\epsilon}_{ij} = \frac{\partial \Omega}{\partial \sigma_{ij}}$$ (2)

$$-\dot{\alpha}_{ij}/h = \frac{\partial \Omega}{\partial \alpha_{ij}} \ .$$ (3)

Here, σ_{ij} and α_{ij} denote the components of the applied and internal stress, respectively. $\dot{\epsilon}_{ij}$ denotes the components of inelastic strain rate and h is a scalar function of the internal stress.

---

* The present treatment concerns only isothermal deformation, extension to nonisothermal conditions follows as in ref. 5.

We further assume, as in references (4-6), that the stress dependence enters through two scalar functions F and G, i.e.,

$$\Omega(F,G) \tag{4}$$

in which

$$F(\Sigma_{ij}) \tag{5}$$

and

$$G(a_{ij}) \tag{6}$$

Σ_{ij} in equation (5) denotes the stress difference

$$\Sigma_{ij} = S_{ij} - a_{ij} , \tag{7}$$

where S_{ij} and a_{ij} represent the deviatoric applied and internal stress, respectively.

As indicated earlier, for a fully isotropic material, F and G can depend only on the respective principal invariants of Σ_{ij} and a_{ij}, i.e.,

$$F(J_2, J_3) \tag{8}$$

and

$$G(\hat{J}_2, \hat{J}_3) \tag{9}$$

where

$$J_2 = \frac{1}{2} \Sigma_{ij} \Sigma_{ji}$$

$$\tag{10}$$

$$J_3 = \frac{1}{3} \Sigma_{ij} \Sigma_{jk} \Sigma_{ki}$$

and

$$\hat{J}_2 = \frac{1}{2} a_{ij} a_{ji}$$

$$\tag{11}$$

$$\hat{J}_3 = \frac{1}{3} a_{ij} a_{jk} a_{ki}$$

Guided by reference (1), we choose particular forms for F and G as

$$F(J_2, J_3) = \frac{(J_2^3 + CJ_3^2)^{1/3}}{K^2} - 1 \qquad (12)$$

$$G(\hat{J}_2, \hat{J}_3) = \frac{(\hat{J}_2^3 + C\hat{J}_3^2)^{1/3}}{K^2} \qquad (13)$$

Here, C indicates the "strength" of the J_3 contribution. Note that for C=0 the functions F and G reduce to the J_2 forms given in references (4 and 5).

Figure 1 shows plots of F=constant in a nondimensional normal/shear stress space for several values of C. Included are the special cases C=0(v.Mises-J_2), C=-4(Tresca) and C=-1.75(Drucker), the latter being the value taken in reference 1 for a yield function in time-independent plasticity. The experimental data points shown in figure 1 were obtained in preliminary experiments for determining the flow surfaces F=constant for a stainless steel (ref. 7). These few data suggest that the time-dependent behavior of this alloy may be somewhat stronger in shear than a J_2 material. A value of C=10 appears to fit the data reasonably well.

Using equations (4), (12), and (13) in equations (2) and (3) gives the flow law,

$$\dot{\varepsilon}_{ij} = f(F)\Gamma_{ij} \qquad (14)$$

in which

$$\Gamma_{ij} = J_2^2 \Sigma_{ij} + \frac{2C}{3} J_3 t_{ij} \qquad (15)$$

and

$$t_{ij} = \Sigma_{ik}\Sigma_{kj} - \frac{2}{3} J_2\delta_{ij} \qquad (16)$$

The evolutionary law becomes

$$\dot{a}_{ij} = h(G)\dot{\varepsilon}_{ij} - r(G) \pi_{ij} \qquad (17)$$

in which

$$\pi_{ij} = \hat{J}_2^2 a_{ij} + \frac{2C}{3} \hat{J}_3 g_{ij} \qquad (18)$$

and

$$g_{ij} = a_{ik}a_{kj} - \frac{2}{3}\hat{J}_2 \delta_{ij} \qquad (19)$$

The functions f(F), h(G) and r(G) can be determined, as in references (4-6), from uniaxial testing. The value of C must be determined from a non-uniaxial test.

CALCULATED RESULTS AND DISCUSSION

Several calculations have been made using forms of the functions, f, h and r and associated material parameters that are typical of ferritic chrome-based and austenitic stainless-steel alloys. Qualitatively similar results can be expected for nickel-based alloys. Figure 2 shows predicted hysteresis loops over a constant strain range ($\Delta\varepsilon$=0.6%) and strain rate ($\dot{\varepsilon}$=.001/m). The curve in figure 2 labeled "uniaxial" can be thought of as having been carefully fit on the basis of uniaxial data. Predictions of pure shear response are also shown, corresponding to different values of C. That based on a J_2 theory is the curve labeled C=0. Even after tedious fitting of uniaxial cyclic data, if the shear prediction does not correlate well with shear data, nothing can be done in a J_2 theory short of compromising the uniaxial correlations. The present J_2, J_3 theory allows some flexibility in accurately predicting response other than uniaxial through the parameter C. Note that the hysteresis loop

labeled C=10, suggested by the data in figure 1, indicates a cyclic response that is about 20% stronger than the J_2 response (C=0).

Figure 3 shows predictions of creep response, i.e., behavior under constant stress. Here, the strain-time curve labeled "uniaxial and shear C=0" represents both the uniaxial response (using the strain scale on the left) and the shear response for a J_2 material (using the strain scale on the right). Each shear response corresponding to a particular value of C is to be measured using the right-hand shear strain scale. In creep, the effect of the J_3 dependence appears to be more pronounced than for strain cycling. Here, for C=10 the creep strain after 100 hours differs by a factor of 2 from that for the J_2 response (C=0).

REFERENCES

1. Drucker, D.C., ASME J. of Appl. Mech., Vol. 16, 1949.

2. Ohasi, Y., and Tanaka, E., ASME J. of Engr. Mat'ls. and Tech., Vol.103, 1981.

3. Chan, K.S., Lindholm, U.S., and Wise, J., ASME J. of Engr. Mat'ls. and Tech., Vol. 107, 1984.

4. Robinson, D.N., et.al., Proc. Specialists Meeting on High-Temp. Design Tech., IAEA, 1976.

5. Robinson, D.N., and Swindeman, R.W., ORNL/TM-8444, 1982.

6. Robinson, D.N., J. Nuc. Engr. and Des., Vol. 96, 1984.

7. Robinson, D.N., and Ellis, J.R., Proc. 5th Internat. Seminar on Inelastic Analysis, Paris, France, 1985.
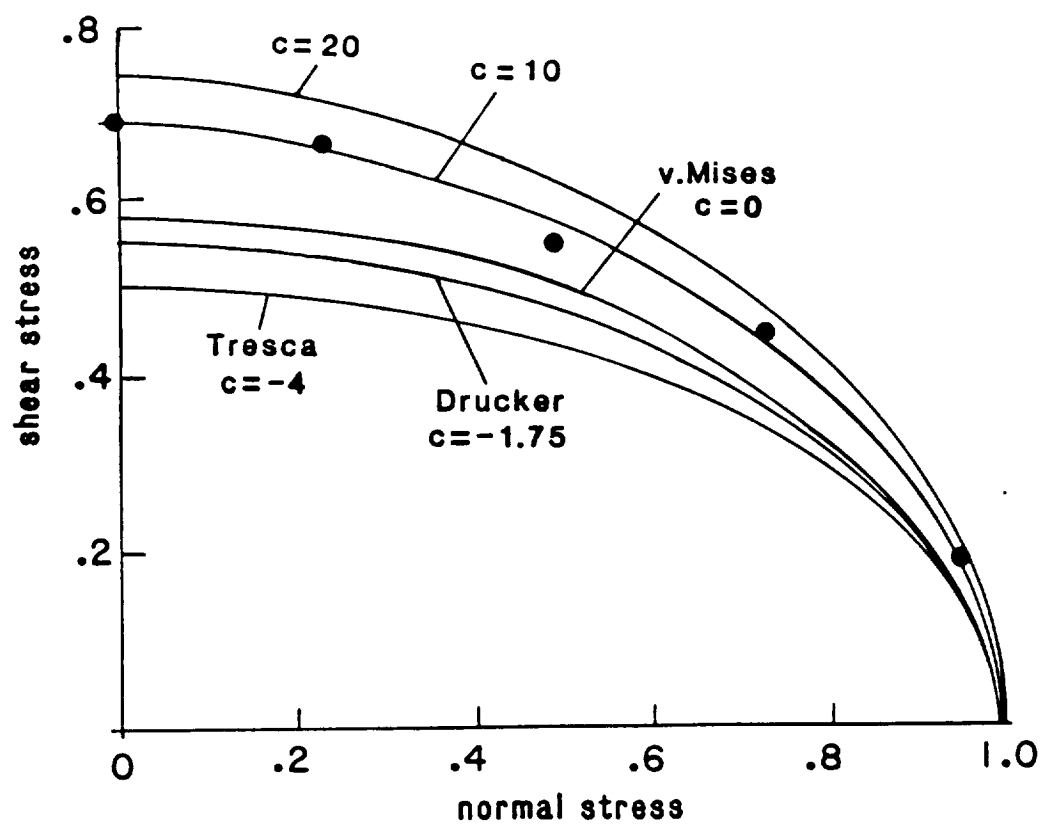
Figure 1   Plots of F=constant in normalized normal/shear
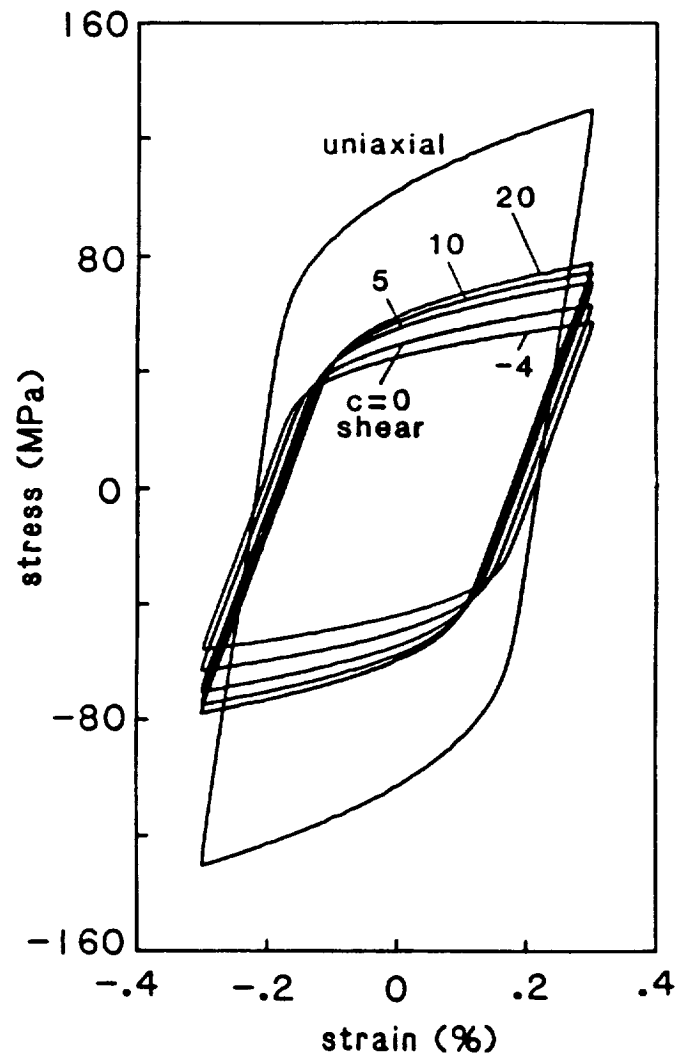stress plane for several values of C.

Figure 2 Saturated hysteresis loops for $\Delta\epsilon=0.6\%$ and $\dot{\epsilon}=.001/m$. Shown is uniaxial response and shear responses for several values of C.
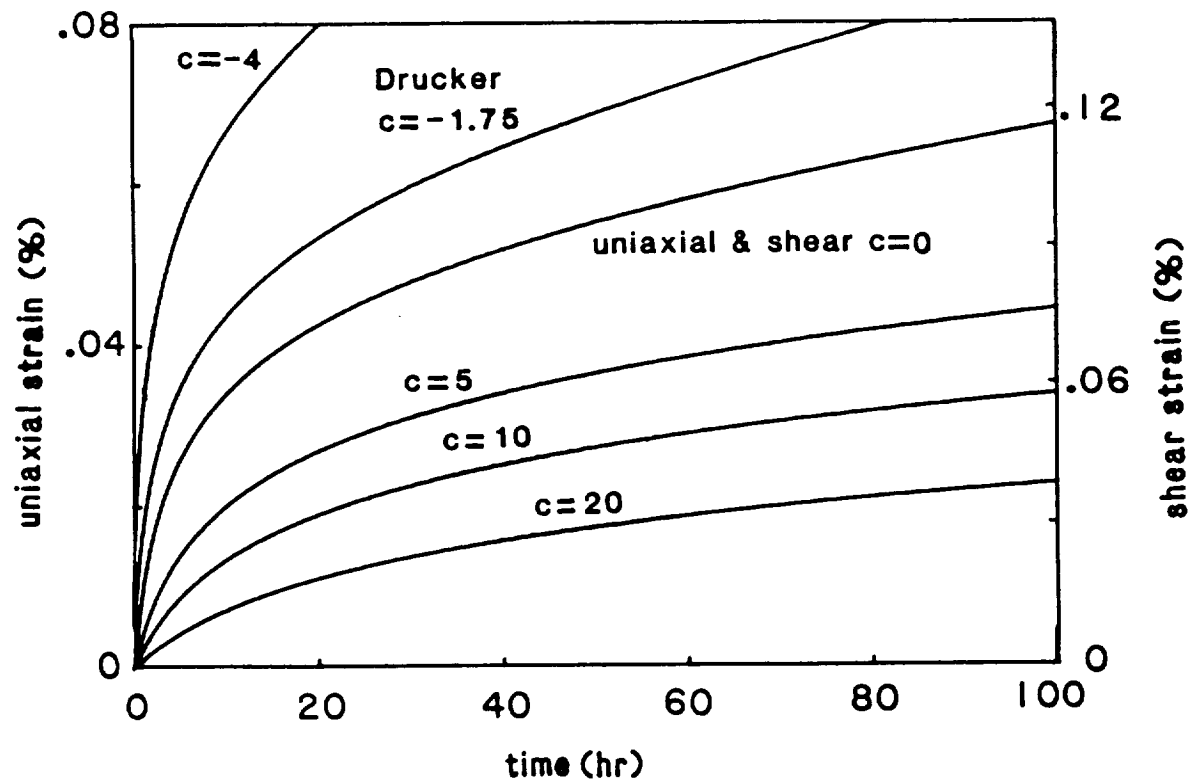
Figure 3 Creep response in uniaxial tension and shear for several values of C.